Available online at www.sciencedirect.com
ScienceDirect
Journal of Power Sources 174 (2007) 1052–1056
JOURNAL OF POWER SOURCES
www.elsevier.com/locate/jpowsour

Short communication

Studies of layered lithium metal oxide anodes in lithium cells

J.T. Vaughey [a], Andrea M. Geyer [a], Nathanael Fackler [b], Christopher S. Johnson [a], K. Edstrom [c], H. Bryngelsson [c], Roy Benedek [a], Michael M. Thackeray [a,*]

[a] *Chemical Engineering Division, Argonne National Laboratory, Argonne, IL 60439, USA*
[b] *Department of Chemistry, Nebraska Wesleyan University, Lincoln, NE 68504, USA*
[c] *Ångstrom Laboratory, Department of Materials Chemistry, Uppsala University, Uppsala, Sweden*

Available online 30 June 2007

Abstract

Numerous efforts have been made to use metal oxides as anode materials for lithium-ion batteries. In this study, we examined layered oxides of the type $LiMO_2$ (M = Co, Ni) and Li_2MO_3 (M = Mn, Mo, Sn) in lithium cells and found them to be electrochemically active while possessing a high capacity. In general, $LiMO_2$ electrodes provide higher reversible capacities than Li_2MO_3 electrodes. First-principles theoretical calculations were used as a guide to determine the most favorable reaction pathway from possible insertion (addition) reactions, decomposition reactions, and metal displacement reactions. For example, using *in situ* X-ray diffraction, $LiCoO_2$ was found to discharge first to CoO and Li_2O (decomposition reaction) and thereafter, upon further reduction, to Co metal and additional Li_2O (displacement reaction). On charging to 3.0 V, only CoO was reformed; the electrode cycled with a reversible capacity of 575 mAh g^{-1}; this reaction pathway is in good agreement with theoretical predictions.

Keywords: Lithium cells; Battery; Anode; Oxides

1. Introduction

Metal oxides have been explored for a number of years as lithium-ion battery anodes. The types of materials studied fall into three main categories: (1) insertion compounds, notably $Li_4Ti_5O_{12}$ [1–4], (2) compounds that act as a source of an active main group metal, e.g. SnO [5–9], and (3) compounds that act as a precursor to form a composite of Li_2O and a catalytic transition metal [10–14]. Each type of material has distinct advantages and disadvantages. For the insertion compound $Li_4Ti_5O_{12}$, high cycling stability is due in part to a negligible crystallographic volume contraction/expansion on lithium insertion/extraction, a flat voltage response at approximately 1.5 V (versus Li), and excellent Li diffusivity [1–3]. Other related lithium titanates, such as $Li_2MTi_6O_{14}$ (M = Sr, Ba), have similar operating voltages and capacities but usually display sloping discharge profiles due in part to the variety of crystallographic sites that are filled during single-phase reaction processes [4]. In contrast, certain main group metal oxides can react with lithium to form a matrix of Li_2O and an electrochemically active main group metal. These composite electrodes tend to offer a high initial capacity below 1 V; however, the reaction that forms the active matrix results in a high irreversible capacity and capacity fade on cycling remains an issue [5–9]. More recently Tarascon and co-workers have evaluated several transition metal oxides, e.g., CoO, in lithium cells [10–14]. As with the main group metal oxides above, these materials work by metal displacement reactions to form lithia and, in this case, a transition metal. On charging to 3.0 V, however, the lithia is formally reduced due to the catalytic activity of the nano-scale transition metal in the electrode matrix, reducing the lithium cations at the counter electrode and reforming the metal oxide. This type of anode affords a stable, high-capacity lithium-ion anode but the 3 V voltage window required for reversibility may be too high for a commercially viable cell [10–14].

Recently Johnson et al. reported the *in situ* formation of lithium-rich metal oxides at low lithium potentials [15,16]. In this work, it was pointed out that certain layered $LiMO_2$ electrodes, such as $Li(Mn_{0.5}Ni_{0.5})O_2$, are able to undergo lithium insertion (addition) to form "di-lithium" materials:

$$Li(Mn_{0.5}Ni_{0.5})O_2 + Li \rightarrow Li_2(Mn_{0.5}Ni_{0.5})O_2$$

For this mixed metal electrode, at cell voltages below 2.0 V, EXAFS studies showed that the formally Mn(IV) ions under-

* Corresponding author. Tel.: +1 630 252 9184; fax: +1 630 252 4176.
E-mail address: thackeray@cmt.anl.gov (M.M. Thackeray).

0378-7753/$ – see front matter © 2007 Elsevier B.V. All rights reserved.
doi:10.1016/j.jpowsour.2007.06.194

went a $2e^-$ reduction directly to Mn(II), producing a layered structure similar to that of Li_2MnO_2 and Li_2NiO_2 [17–19]. A similar insertion mechanism has been speculated for the layered lithium ruthenate Li_2RuO_3, or $Li(Li_{0.33}Ru_{0.67})O_2$, where a reversible plateau around 2.0 V versus lithium was observed [20]. In this study, we have evaluated a number of layered $LiMO_2$ (M = Co, Ni) and Li_2MO_3 (M = Mn, Mo, Sn) compounds as possible lithium-ion battery anodes, with a focus on determining the controlling mechanisms that occur during discharge and charge.

2. Experimental

The metal oxides $LiMO_2$ (M = Co, Ni) and Li_2MO_3 (M = Mn, Mo, Sn) were synthesized directly by solid-state reactions at elevated temperatures. The materials $LiCoO_2$, $LiNiO_2$, and Li_2MnO_3 were made by heating well mixed, stoichiometric amounts of $LiOH{\cdot}H_2O$ (Aldrich, 98%) and $Co(OH)_2$, $Ni(OH)_2$, or $Mn(OAc)_2$ (Aldrich, 99.9%), respectively, in air at 700 °C and slow cooling to room temperature. The nickel and cobalt hydroxide precursors were synthesized by the addition of ammonium hydroxide to a solution of the nitrate salts, followed by filtering and drying. Li_2MoO_3 was made by reacting stoichiometric amounts of MoO_3 (Aldrich, 99.5%) and $LiOH{\cdot}H_2O$ under a 4% hydrogen atmosphere for 24 h at 700 °C, whereas Li_2SnO_3 was made by dry mixing Li_2CO_3 (Aldrich, 99%) and SnC_2O_4 (Aldrich, 98%) overnight, followed by heating for 12 h at 900 °C. All the samples were determined by powder X-ray diffraction (XRD) to be single-phase. In-situ XRD data of a $LiCoO_2$ electrode were collected from a Li/$LiCoO_2$ electrochemical cell using methods and an experimental design reported previously [21].

The $LiMO_2$ and Li_2MO_3 electrode powders were ground, sieved, and subsequently mixed with 10 wt% acetylene black and 10 wt% polyvinylidenedifluoride (PVDF) binder in *N*-methylpyrrolidone (NMP) solvent. The electrode mixture was then laminated onto copper foil, dried at 75 °C for 1 h in air and vacuum-dried at 120 °C for 6 h before use. Electrochemical coin cells were constructed in an argon-filled glove-box using lithium as the negative electrode. The electrodes were separated by a Celgard separator; the electrolyte was a 1 M $LiPF_6$ solution in a 1:1 by weight mixture of ethylene carbonate (EC)/diethyl carbonate (DEC). Cells were cycled under a constant current of 0.1 mA.

Theoretical modeling of possible reaction mechanisms was undertaken by methods described previously [22]. Reaction mechanisms considered included lithium insertion (addition), decomposition and metal displacement.

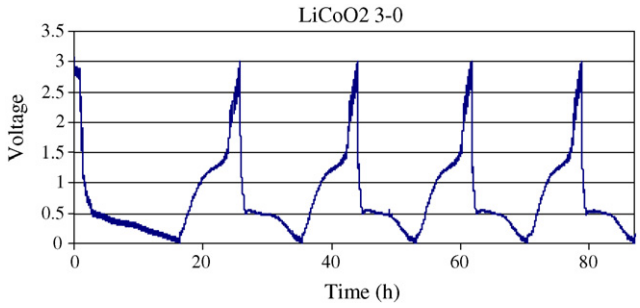

Fig. 2. The cycling profiles of the first 5 cycles of a Li/$LiCoO_2$ cell cycled between 0 and 3 V.

3. Results and discussion

Alternative anodes to graphite for lithium batteries have been sought for several years, driven by a desire to increase capacity and abuse tolerance. Although significant effort has gone into studying a variety of main group metal-based systems, e.g. Cu_6Sn_5, Al, Si/C, no single system has yet been able to replace graphite as the anode material of choice [23–26]. In this work, we evaluated the layered lithium metal oxides $LiCoO_2$, $LiNiO_2$, Li_2MnO_3, Li_2SnO_3, and Li_2MoO_3 as anode materials for lithium-ion batteries. The layered $LiMO_2$, Li_2MO_3 and Li_2MO_2 structure types described in this work are shown in Fig. 1a–c, respectively.

3.1. Li/$LiMO_2$ cells

Two layered rock-salt-type (α-$NaFeO_2$) electrode materials, $LiCoO_2$ and $LiNiO_2$ (Fig. 1a) were evaluated. Fig. 2 shows the voltage versus time plot for the Li/$LiCoO_2$ cell. Lithium reacts with $LiCoO_2$ at approximately 0.5 V on discharge, whereas most of the lithium is removed at around 1.2 V on charge. The initial capacity delivered to 0 V corresponded to ~1200 mAh g^{-1} (4.4 Li per $LiCoO_2$ formula unit), whereas only ~575 mAh g^{-1} (2.1 Li) could be cycled reversibly. The excess capacity delivered during the first cycle has been studied extensively by Tarascon and co-workers and is believed to result from formation of an unusually thick SEI layer on the electrode surface, possibly due to the catalytic activity of the displaced Co metal with the electrolyte [13,14]. A capacity versus cycle number plot in Fig. 3 shows that after the initial few cycles the charge/discharge capacity (~575 mAh g^{-1}) is extremely stable for 50 cycles.

Literature reports have shown that CoO provides a reversible capacity of 800 mAh g^{-1}, that lithium insertion into the oxygen array occurs on discharge at 1.2 V, and that lithium removal on charge occurs at 2.0 V; X-ray diffraction studies revealed

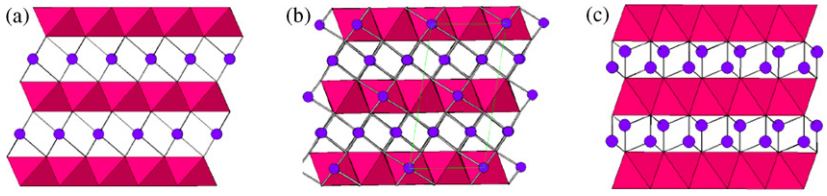

Fig. 1. The structures of (a) $LiMO_2$, (b) Li_2MO_3, and (c) Li_2MO_2. The polyhedra contain the M-metal in octahedral coordination, the Li are shown as spheres.

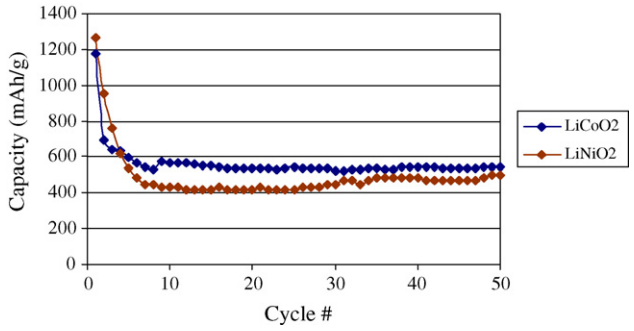

Fig. 3. The first 50 cycles of the two $LiMO_2$ (M = Co, Ni) materials.

that CoO re-forms on charging by reaction of cobalt metal with its surrounding lithia matrix [13]. For $LiCoO_2$, our *in situ* XRD data collected after an initial discharge to 0 V and subsequent charge to 1.5 V indicate that the predominant reaction, which occurs between 1.0 and 1.5 V on charge, corresponds to the formation of CoO, presumably from the reaction of cobalt and Li_2O. The XRD patterns of the initial $LiCoO_2$ electrode (OCV = 3.0 V) prior to discharge and after the initial charge to 1.5 V are shown in Fig. 4. The lower voltage for the discharge reactions of Li/$LiCoO_2$ cells compared with the literature values for Li/CoO cells is attributed, in part, to an overpotential in the envisaged initial decomposition reaction for the Li/$LiCoO_2$ cells, namely

$$Li + LiCoO_2 \rightarrow CoO + Li_2O$$

that yields two insulating products and occurs prior to the metal displacement reaction that typifies the discharge of Li/CoO cells, namely

$$2Li + CoO \rightarrow Co + Li_2O$$

In this respect, note also that there is twice as much displaced Co per Li_2O in discharged Li/CoO cells compared with discharged Li/$LiCoO_2$ cells, which could provide superior electronic conductivity to these electrodes compared with discharged $LiCoO_2$ electrodes [27].

The $LiNiO_2$ electrode cycles in a manner similar to that of $LiCoO_2$. On the initial discharge to 0 V, the electrode yields 1275 mAh g^{-1} (4.6 Li/$LiNiO_2$) and on cycling stabilizes at a reversible capacity of ~450 mAh g^{-1} (1.6 Li/$LiNiO_2$). Therefore, by analogy to $LiCoO_2$, it appears that the stable binary oxide NiO, which is isostructural with CoO, is most likely a major component of the electrode; in this case, however, the gradual increase in capacity on cycling, as shown in the first 50 cycles (Fig. 3) indicates that several break-in cycles were required to fully utilize the electrode material.

The initial discharge capacity delivered by both $LiCoO_2$ and $LiNiO_2$ electrodes (1200–1275 mAh g^{-1}, respectively) was significantly higher than their theoretical values for the reduction of the trivalent cobalt and nickel ions to the metallic state (822 and 824 mAh g^{-1}, respectively). The excess capacity has been attributed by Tarascon and co-workers to the formation of an electrochemically active lithium-containing SEI layer induced by the reaction of the displaced Co and nickel metals with the electrolyte solvents [10–14]. These authors have suggested that, on cycling, this low-voltage side reaction eventually forms PEO-like oligomers that may influence the long-term performance of Li/metal oxide cells [12].

3.2. *Li/Li_2MO_3 cells*

With recent evidence that lithium may be inserted electrochemically into the lithium-rich rock-salt phase Li_2RuO_3 at low potentials, we initiated preliminary studies of several other layered Li_2MO_3 compounds (Fig. 1b) as anode materials (M = Mn, Mo, Sn) [28].

As with many other oxide anode materials, large capacities were delivered by the Li_2MO_3 electrodes on the initial discharge to 0 V, and an unacceptably high inefficiency dominated the initial discharge/charge cycle. None of the Li_2MO_3 materials investigated in this study showed sufficiently high capacity retention or cycling efficiency, as shown in Fig. 5, to suggest that there were reversible phenomena of practical interest to warrant further study of these reactions at low potentials. It was evident, however, particularly from the electrochemical data of Li/Li_2MoO_3 cells (Fig. 6) and ex situ XRD data of cycled Li_2MoO_3 electrodes (not shown), that the parent electrode structures were destroyed on electrochemical cycling to yield products that were amorphous to X-rays. Whereas the limited capacity delivered by Li_2MnO_3 and Li_2MoO_3 electrodes was attributed to redox reactions involving the transition metal ions, the capacity of the Li_2SnO_3 electrode, much of which was delivered below 400 mV (Fig. 7), was attributed to the Li_xSn alloying reactions of Zintl phases within an essentially inert Li_2O

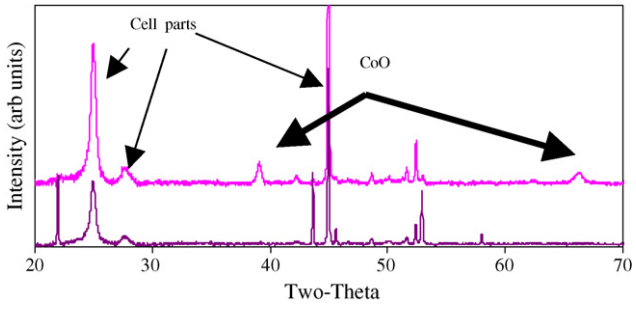

Fig. 4. *In situ* XRD of a $LiCoO_2$ electrode at two different states of charge. The bottom XRD pattern was collected at 3.0 V, before the initial discharge; the top pattern was recorded at 1.5 V after the initial charge.

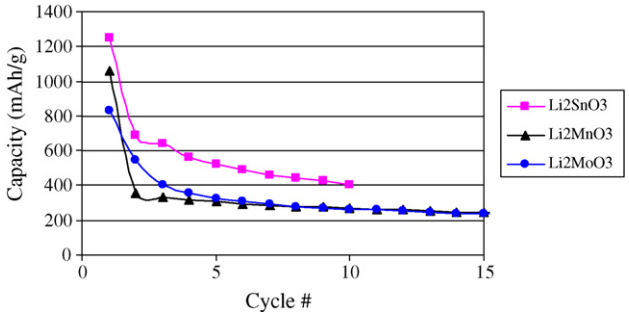

Fig. 5. Capacity vs. cycle number plots of the three Li/Li_2MO_3 cells (M = Sn, Mn, Mo).

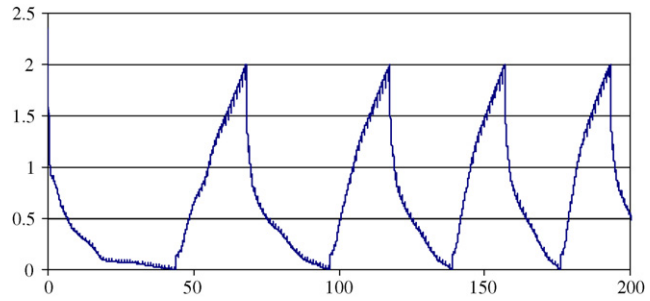

Fig. 6. The first four cycles of a Li/Li_2MoO_3 cell in the voltage window 0–2 V.

matrix as described for other tin oxide-based anode materials [29,30].

3.3. Theoretical modeling of $LiMO_2$ electrode reactions

Both the voltage and the capacity retention of an electrode material depend on the detailed path adopted in its reaction with lithium. Since the reaction path depends on kinetic factors, such as lithium diffusion and cell current rates, in addition to thermodynamic factors, the true reaction path is difficult to predict accurately.

The experimental results obtained in this work for layered structures with composition $LiMO_2$ and trigonal symmetry ($R-3m$), in conjunction with first-principles calculations described in detail elsewhere [31,32], provide some guidelines as to the reactions that occur in these materials. Three general types of reactions come into consideration: (1) the addition reaction, in which additional Li intercalates into the layered host structure to form a hexagonally-close-packed (P−3m1) Li_2MO_2 structure (Fig. 1c); (2) the decomposition reaction, in which metal oxide and Li_2O are formed; and (3) the displacement reaction, in which metal and Li_2O are formed. Recently, a first-principles investigation of these reactions for layered $LiMO_2$ with M = Mn, Co and Ni, as well as equiatomic pseudo-binary mixtures, was performed [32]. For all of these compounds, the decomposition reaction was energetically preferred over the displacement and addition reactions, but the difference between the most and least preferred was less than about 20 percent. In the case of M = ($Mn_{0.5}Ni_{0.5}$), which is known to undergo an addition reaction, a voltage of 2.2 V was predicted, whereas the measured value was about 1.8 V. The structural transformation from an

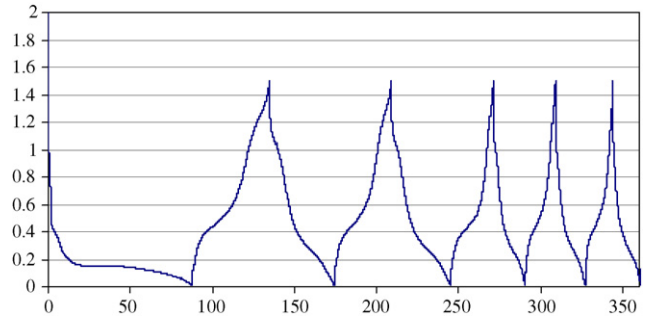

Fig. 7. The first five cycles of a typical Li/Li_2SnO_3 cell in the voltage window 0–1.5 V.

$R-3m$ structure of Li($Mn_{0.5}Ni_{0.5}$)O_2 to the P−3m1 structure of Li_2($Mn_{0.5}Ni_{0.5}$)O_2 is expected to be at least partially responsible for the overprediction; the measured voltage may reflect a structure that is intermediate between $R-3m$ and P−3m1. Nevertheless, the predicted voltage for the Li addition reaction with Li($Mn_{0.5}Ni_{0.5}$)O_2 is still reasonably close to the experimentally measured voltage, and the agreement of first-principles calculation with experiment is even closer for intercalation reactions in which no structural change of the host occurs [17].

The behavior for $LiCoO_2$ strongly contrasts with that of Li($Mn_{0.5}Ni_{0.5}$)O_2. As mentioned earlier, the measured potential for discharge of the former electrode is 0.5 V versus Li^0, far lower than the predicted voltage for the addition reaction, 2.4 V [33]. This behavior suggests that the addition of Li to $LiCoO_2$ results initially in a decomposition reaction (to form CoO and Li_2O) prior to a displacement reaction in which cobalt is extruded from the close-packed oxygen array. The decomposition and displacement reactions are accompanied by profound changes in the host atomic structure, and the measured voltage may be characteristic of unknown intermediate structures rather than the final products. As a result, the measured voltage falls below the thermodynamic reaction energies predicted for the addition, decomposition or displacement reactions. This, we believe, accounts for the marked difference in the measured voltages for Li($Mn_{0.5}Ni_{0.5}$)O_2 and $LiCoO_2$.

For Li/$LiNiO_2$ cells, a voltage plateau on the first discharge is observed at about 0.9 V which, based on the above considerations, seems to preclude an addition reaction; we therefore attribute this process to a decomposition reaction that occurs prior to the displacement of metallic nickel, similar to that observed in Li/$LiCoO_2$ cells.

Therefore, for systems with layered $LiMO_2$ structures we find two basic behaviors upon initial lithiation. We conclude that when an addition reaction occurs, the discharge voltage is approximately 2 V, whereas decomposition reactions occur at voltages typically less than 1 V prior to the extrusion of M cations from the oxide lattice.

4. Conclusions

A series of layered $LiMO_2$ and Li_2MO_3 metal oxides have been evaluated in Li/$LiMO_2$ and Li/Li_2MO_3 cells in the search for new lithium battery anodes. In general, both types of materials provide a high initial capacity on reaction with lithium but suffer from a large first-cycle irreversible capacity. $LiMO_2$ electrodes provide higher reversible capacities on cycling than do Li_2MO_3 electrodes; they appear to cycle in a manner similar to the mechanism proposed by Tarascon's group. Theoretical modeling of the reactions between lithium and $LiCoO_2$, in particular, supports experimental results that suggest a decomposition reaction occurs that generates a lower valent metal oxide (CoO) as an intermediary step in the reaction prior to the reduction to Co metal. In this study, several other related or isostructural materials, including $LiCrO_2$, $LiTiO_2$, $LiMoO_2$, Li_2TiO_3, Li_2ZrO_3, were also evaluated but they showed either no significant electrochemical reaction or reversibility with lithium.

Acknowledgments

The authors gratefully acknowledge support from the Office of FreedomCar and Vehicle Technologies of the U.S. Department of Energy.

"The submitted manuscript has been created by the University of Chicago as Operator of Argonne National Laboratory ("Argonne") under Contract No. W-31-109-ENG-38 with the U.S. Department of Energy. The U.S. Government retains for itself, and others acting on its behalf, a paid-up, nonexclusive, irrevocable worldwide license in said article to reproduce, prepare derivative works, distribute copies to the public, and perform publicly and display publicly, by or on behalf of the Government."

References

[1] E. Ferg, R.J. Gummow, A. DeKock, M.M. Thackeray, J. Electrochem. Soc. 141 (1994) L147.
[2] K. Zaghib, M. Simoneau, M. Armand, M. Gauthier, J. Power Sources 81 (1999) 300.
[3] C.H. Chen, J.T. Vaughey, A.N. Jansen, D.W. Dees, A.J. Kahaian, T. Goacher, M.M. Thackeray, J. Electrochem. Soc. 148 (2001) A102.
[4] I. Belharouak, K. Amine, Electrochem. Commun. 5 (2003) 435.
[5] H. Morimoto, M. Nakai, M. Tatsumisago, T. Minami, J. Electrochem. Soc. 146 (1999) 3970.
[6] J. Yang, Y. Takeda, N. Imanishi, J.Y. Xie, O. Yamamoto, J. Power Sources 97–98 (2001) 216.
[7] J. Read, D. Foster, J. Wolfenstine, W. Behl, J. Power Sources 96 (2001) 277.
[8] M. Mohamedi, S.J. Lee, D. Takahashi, M. Nishizawa, T. Itoh, I. Uchida, Electrochim. Acta 46 (2001) 1161.
[9] H.Y. Lee, S.M. Lee, Electrochem. Commun. 6 (2004) 465.
[10] F. Badway, I. Plitz, S. Grugeon, S. Laruelle, M. Dolle, A.S. Gozdz, J.M. Tarascon, Electrochem. Solid State Lett. 5 (2002) A115.
[11] V. Pralong, J.B. Leriche, B. Beaudoin, E. Naudin, M. Morcette, J.M. Tarascon, Solid State Ionics 166 (2004) 295.
[12] R. Dedrvere, S. Laruelle, S. Grugeon, P. Poizot, D. Gonbeau, J.M. Tarascon, Chem. Mater. 16 (2004) 1056.
[13] P. Poizot, S. Laruelle, S. Grugeon, L. Dupont, J.M. Tarascon, Nature 407 (2000) 496.
[14] P. Poizot, S. Laruelle, S. Grugeon, J.M. Tarascon, J. Electrochem. Soc. 149 (2002) A1212.
[15] C.S. Johnson, J.S. Kim, A.J. Kropf, A.J. Kahaian, J.T. Vaughey, L.M.L. Fransson, L.M.L.K. Edstrom, M.M. Thackeray, Chem. Mater. 15 (2003) 2313.
[16] C.S. Johnson, J.S. Kim, A.J. Kropf, A.J. Kahaian, J.T. Vaughey, M.M. Thackeray, Electrochem. Commun. 4 (2002) 492.
[17] W.I.F. David, J.B. Goodenough, M.M. Thackeray, J.M. Thomas, Rev. Chim. Miner. 20 (1983) 636.
[18] J.R. Dahn, U. Von Sacken, C.A. Michal, Solid State Ionics 44 (1990) 87.
[19] I. Davidson, J.E. Greeden, U. Von Sacken, C.A. Michal, J.R. Dahn, Solid State Ionics 46 (1991) 243.
[20] G.J. Moore, C.S. Johnson, M.M. Thackeray, J. Power Sources 119 (2003) 216.
[21] O. Bergström, T. Gustafsson, J.O. Thomas, J. Appl. Crystallogr. 31 (1998) 103.
[22] R. Benedek, J.T. Vaughey, M.M. Thackeray, Chem. Mater. 18 (2006) 1713.
[23] K.D. Kepler, J.T. Vaughey, M.M. Thackeray, Electrochem. Solid State Lett. 2 (1999) 307.
[24] Q.F. Li, N.J. Bjerrum, J. Power Sources 110 (2002) 1.
[25] I.S. Kim, P.N. Kumta, J. Power Sources 136 (2004) 145.
[26] L.M.L. Fransson, J.T. Vaughey, R. Benedek, K. Edstrom, J.O. Thomas, M.M. Thackeray, Electrochem. Commun. 3 (2001) 317.
[27] C.D. May, J.T. Vaughey, Electrochem. Commun. 6 (2004) 1075.
[28] V. Massarotti, M. Bini, D. Capsoni, A. Altomare, G.G.A. Molterni, J. Appl. Crystallogr. 30 (1997) 123.
[29] C. Lupu, J.G. Mao, J.W. Rabalais, A.M. Guloy, J.W. Richardson, Inorg. Chem. 42 (2003) 3765.
[30] T. Brousse, S.M. Lee, L. Pasquereau, D. Defives, D.M. Schleich, Solid State Ionics 115 (1998) 51.
[31] V.B. Nalbandyan, Russ. J. Inorg. Chem. 45 (2000) 1652.
[32] F. Zhou, M. Cococcioni, C.A. Marianetti, D. Morgan, G. Ceder, Phys. Rev. B 70 (2004) 235121.
[33] K. Kang, C.H. Chen, B.J. Hwang, G. Ceder, Chem. Mater. 16 (2004) 2685.